clone on 11 February only 30 km south of Tongatapu (the main island of Tonga). Gita affected multiple island nations and territories in its path. Tonga was the hardest hit, with severe damage occurring on the islands of Tongatapu and 'Eua including two fatalities and 41 injuries, as well as thousands of damaged structures. Agriculture was devastated on the two islands. The Tongan parliament building, more than 100 years old, was flattened. Gita was the strongest storm to impact Tonga since modern records began in the 1960s. According to the Ministry of Finance and National Planning, Gita inflicted $158 million (U.S. dollars) worth of damage, making it the costliest storm in their national history. Torrential rain and damaging wind impacted Samoa, American Samoa, and Fiji's Lau group. Wallis and Futuna, Niue, and Vanuatu were also affected. A state of emergency was declared for multiple districts on New Zealand's South Island as flooding, landslides, and high winds closed roads and damaged buildings, and $35.6 million NZ dollars ($24.3 million U.S. dollars) worth of insured damage occurred. Gita's peak 10-min sustained wind speeds were 111 kt (57 m s^{-1}); its minimum central pressure was 927 hPa.

Gita was followed by the second severe cyclone of the season, Hola, which formed as a tropical disturbance to the northeast of Fiji on 3 March. Hola was classified as a Category 1 cyclone on 6 March. One day later, Hola was classified as a Category 4 cyclone with 10-min sustained winds of 89 kt (46 m s^{-1}) and a minimum central pressure of 952 hPa. Hola brought severe winds to Vanuatu, destroying multiple buildings. Falling trees caused one fatality on Pentecost Island, and two children on Santo Island drowned after they were washed away by a flooded river. Hola caused minimal damage in New Caledonia and flights to be cancelled in New Zealand.

On 11 March, the Fiji Meteorological Service reported that a tropical disturbance had developed to the southwest of the Solomon Islands. As the storm moved south, it strengthened into a Category 1 cyclone named Linda. Linda attained its peak intensity on 13 March, with 10-min sustained winds of 40 kt (21 m s^{-1}) and a minimum central pressure of 993 hPa. While Cyclone Linda was not long-lived, the deteriorating vestiges of this storm system passed near Fraser Island (Queensland, Australia) about a week later and produced large waves and swell, while the mainland near the Sunshine Coast experienced waves of up to 8 m. Cyclone Iris formed as a tropical disturbance on 20 March over the eastern Solomon Islands. It was classified as an Australian Category 1 cyclone on 24 March. Iris' peak 10-min sustained winds (while it was in the Southwest Pacific basin) were 40 kt (21 m s^{-1}), and its minimum central pressure was 993 hPa.

On 23 March, a Category 1 tropical cyclone emerged into the Southwest Pacific basin just west of the Gulf of Carpentaria (Australia) and was named Nora by the Australian Bureau of Meteorology. Within a couple of days, Nora intensified into a Category 3 severe cyclone and tracked to the southeast before making landfall on the Cape York Peninsula at Category 3 strength. Afterward, Nora gradually weakened, degenerating into a tropical low soon afterward. On 26 March, Nora's remnant low stalled and slowly meandered counterclockwise over the Top End of the Northern Territory. On 27 March, Nora's remnant moved westward across the Gulf of Carpentaria before making landfall on the Australian coast and dissipating. Nora's peak 10-min wind speed was 84 kt (43 m s^{-1}), and its minimum central pressure was 958 hPa.

Cyclone Josie achieved Category 1 status on 31 March. The storm passed to the south of Fiji's main islands. Despite not making landfall, the storm caused heavy rainfall and sustained gale-force winds in Viti Levu. In addition, severe flooding occurred around Nadi and Ba, causing significant property and crop damage. At least six people were killed. More than 70 roads were closed due to flooding, mostly in the Western Division of Viti Levu. Josie's peak 10-min wind speed was 40 kt (21 m s^{-1}), and its minimum central pressure was 993 hPa.

Severe Cyclone Keni affected Fiji about a week after Cyclone Josie had passed. It was classified as a Category 3 Severe Cyclone on 10 April and had peak 10-min sustained wind speeds of 76 kt (39 m s^{-1}) and a minimum central pressure of 970 hPa. Cyclone Keni caused the most damage on the island of Kadavu in the Eastern Division, with flooding and high winds destroying houses and crops. Keni was the last named cyclone of the season.

g. Tropical cyclone heat potential—R. Domingues, G. J. Goni, J. A. Knaff, I.-I. Lin, and F. Bringas

Changes in upper-ocean thermal conditions observed within the seven TC basins are described here, focusing on vertically integrated conditions observed during the 2018 TC season with respect to the long-term mean and to values observed during 2017. To accomplish this, the tropical cyclone heat potential (TCHP; e.g. Goni et al. 2017), defined as the excess heat content stored in the water column between the sea surface and the depth of the 26°C isotherm, is used as a key parameter in this assessment.

The TCHP provides a metric for evaluating the heat content in upper-ocean layers, which may modulate the effective SST under a TC and affect the air–sea latent and sensible heat fluxes that can lead to storm intensification (Mainelli et al. 2008; Lin et al. 2013). For example, values of TCHP above 50 kJ cm^{-2} have been associated with the intensification of North Atlantic hurricanes when favorable atmospheric conditions were also present (e.g., Shay et al. 2000; Mainelli et al. 2008; Lin et al. 2014).

Year-to-year variations in TCHP during 2018 are described here based on anomalies (from the 1993–2018 mean values, Fig. 4.35) for the primary months of TC activity in each hemisphere: June–November 2018 in the Northern Hemisphere, and November 2017–April 2018 in the Southern Hemisphere. In addition, differences in TCHP between the 2018 and 2017 seasons are also displayed (Fig. 4.36). Generally, TCHP anomalies show large spatial and temporal variability within and among the TC basins associated mainly with oceanic mesoscale features, year-to-year variability (e.g., ENSO), or long-term decadal variability. Sustained ocean monitoring based on both satellite altimetry and in situ observations allows for a reliable assessment of ocean variability on various timescales (e.g., Lin et al. 2008; Goni et al. 2009; Goni and Knaff 2009; Pun et al. 2013).

During the 2018 season, above-normal TCHP anomalies were observed in portions of all basins. These conditions in some of the basins provided favorable ocean conditions for the intensification of TCs. Negative TCHP anomalies were observed mostly in the eastern part of the North Atlantic basin, in the southern part of the western North Pacific basin, the South Indian Ocean, and the southwest Pacific basin. Differences in the TCHP values between the 2018 and 2017 seasons (Fig. 4.36) indicate that five of the seven basins exhibited a decrease in upper-ocean heat content during 2018 compared to conditions observed in 2017. The two notable exceptions were the western North Atlantic (including the Gulf of Mexico) and the eastern North Pacific basins.

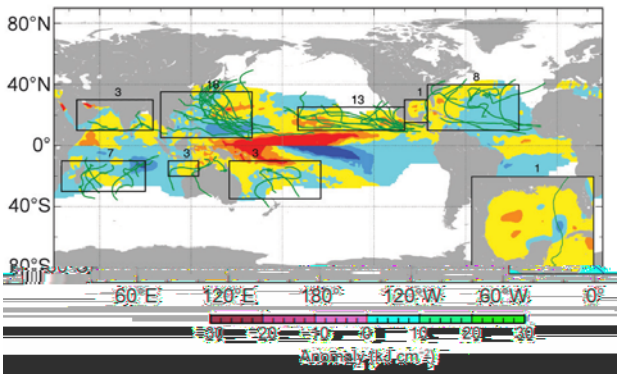

Fig. 4.35. Global anomalies of TCHP (kJ cm^{-2}) during 2018. The boxes indicate the seven regions where TCs occur: from left to right, southwest Indian, North Indian, western North Pacific, Australian region, southwest Pacific, eastern North Pacific, and North Atlantic (shown as Gulf of Mexico and tropical Atlantic separately). Green lines indicate the trajectories of all TCs reaching at least Saffir–Simpson Category 1 during Nov 2017–Apr 2018 in the SH and Jun–Nov 2018 in the NH. The numbers above each box correspond to the number of Category 1 and above cyclones that traveled within each box. Gulf of Mexico conditions are shown in the inset in the lower right corner.

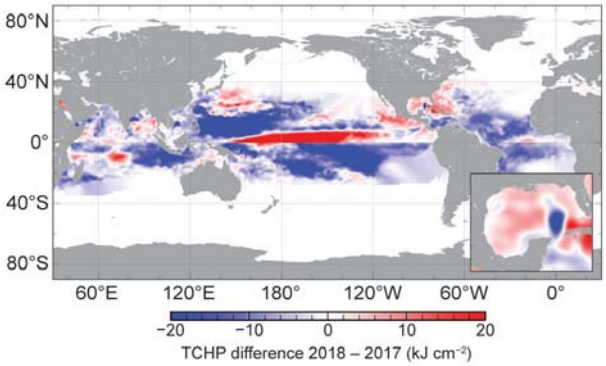

Fig. 4.36. TCHP differences (kJ cm^{-2}) between 2018 and 2017.

In the eastern part of the North Atlantic basin, TCHP values were ~10 kJ cm^{-2} (10%–30%) below the long-term average (Fig. 4.35). In the western part of the basin, TCHP values were 10–20 kJ cm^{-2} (10%–40%) above the long-term average (Fig. 4.35). Associated with these conditions, above-normal TC activity was observed in the North Atlantic for the third consecutive year (Section 4f2). In particular, the warmer-than-usual upper-ocean conditions in the western part of the North Atlantic basin (including the Gulf of Mexico), with TCHP values up to 40% larger than the long-term average, likely provided favorable oceanic conditions for the rapid intensification of Hurricanes Florence (31 August–17 September) and Michael (7–12 October). Oceanic conditions observed during Hurricane Michael, the strongest Atlantic hurricane in 2018, are examined in more detail in Sidebar 4.2.

In the North Pacific, upper-ocean thermal conditions were largely modulated by the transition toward weak El Niño in the third and fourth quarters of 2018 (Section 4b), with warmer waters in the eastern North Pacific (ENP) basin and slightly cooler waters in the western North Pacific (WNP) basin (Fig. 4.36). Upper-ocean thermal conditions, evaluated in terms of TCHP values, are closely modulated by ENSO variability in both the ENP and WNP basins (Lin et

al. 2014; Zheng et al. 2015). In the ENP basin, TCHP values during 2018 were greater than those observed in 2017 (Fig. 4.36) and were 10–20 kJ cm^{-2} larger than the long-term average (Fig. 4.35), which represents an increase of 20%–40%. The substantially larger-than-usual TCHP conditions in this basin provided favorable upper ocean conditions for the 2018 ENP hurricane season—especially west of 140°W and near the Hawaiian Islands, which was characterized by record-breaking levels of TC activity (Section 4f3).

Despite exhibiting lower-than-usual TCHP conditions during the 2018 season (Fig. 4.35), TC activity in the WNP basin was above average (section 4f4). This is because the total number of TCs in the WNP is more closely related to atmospheric dynamics (Lin and Chan 2015) than to upper-ocean thermal conditions. In addition, although lower than in 2017, TCHP values during 2018 were consistently larger than 80 kJ cm^{-2}. This provided conditions that were sufficiently warm for TC intensification in most parts of the basin. Among the notable Category 5 TCs recorded, Super Typhoons Mangkhut (7–17 September) and Yutu (21 October–2 November) each reached a peak intensity of 155 kt (80 m s^{-1}) sustained winds and were the most intense TCs globally in 2018. Both Mangkhut and Yutu reached Category 5 status while traveling over the WNP's Main Development Region, which is characterized by large TCHP values (Lin et al. 2013; 2014). In fact, Mangkhut reached peak intensity and maintained Category 5 status for 3.5 days while traveling over this area, where the TCHP had values larger than 120 kJ cm^{-2}.

In the North Indian Ocean basin, average TCHP values observed during the 2018 cyclone season were 10 kJ cm^{-2} (~10%) larger than the long-term average (Fig. 4.35), and slightly lower than 2017 conditions. In the Bay of Bengal, TCHP values were consistently larger than 70 kJ cm^{-2}, while values above 50 kJ cm^{-2} were observed in most of the Arabian Sea. The warmer-than-usual conditions in this basin likely favored an above-average number (eight) of TC formations during the 2018 season, which was the most active North Indian Ocean season since 1992. In the South Indian basin, TCHP values below the long-term mean by 10–20 kJ cm^{-2} likely contributed to a below-average season.

In summary, 2018 was characterized by higher-than-normal values of TCHP in the western part of the North Atlantic basin, in the eastern North Pacific basin, and in the North Indian basin. Larger-than-usual ocean heat content in these basins likely contributed to both the above-normal TC activity and the intensity of TCs recorded there. Upper-ocean heat content conditions in both the ENP and WNP basins were largely modulated by the onset of weak El Niño conditions late in 2018 (see Section 4b). Overall, TCHP anomalies observed in 2018 were not as large as anomalies observed in 2017. Targeted ocean observations during 2018 indicated that upper-ocean conditions favored the intensification of several major TCs.

SIDEBAR 4.2: UPPER-OCEAN CONDITIONS IN THE GULF OF MEXICO DURING HURRICANE MICHAEL—G. J. GONI AND R. DOMINGUES

The Gulf of Mexico's upper-ocean circulation is dominated by the presence of the Loop Current, which often intrudes far into the Gulf and sheds warm, anticyclonic rings and smaller eddies. Coastal waters are heavily influenced by riverine outflow that may reach areas hundreds of kilometers away from their source. Upper-ocean conditions have been linked to the intensification of several hurricanes in the Gulf. For example, Hurricanes Opal (1995; Shay et al. 2000) and Katrina (2005; Goni et al. 2017) both intensified while traveling in the Gulf of Mexico over a warm eddy and a Loop Current ring, respectively.

Hurricane Michael, which traversed the Caribbean Sea and then the Gulf of Mexico during October 2018, was characterized by its steady intensification rate and its extremely intense landfall intensity in the Florida Panhandle (Sidebar 4.1). The relevant upper-ocean conditions in the Gulf of Mexico during this period can be described in terms of the geostrophic velocity and sea surface height, SST, tropical cyclone heat potential (upper-ocean heat content), and upper-ocean salinity for pre-storm conditions at the beginning of October 2018 (Fig. SB4.3, four panels). These fields indicate that the Loop Current during early October was retracted to the south, and a warm Loop Current anticyclonic ring was centered around 88°W, 25°N, as shown by the surface height fields and also confirmed by surface drifters (not shown). As an aside, this particular location of the Loop Current is also important for the Gulf and southeast Florida ecosystems.